

# Friction Modelling in Particle-to-Particle Contact

J.C. Campbell, T. De Vuyst, R. Vignjevic, N. Djordjevic, K. Hughes  
 Dynamic Response Group, Structural Integrity Theme, Brunel University London  
 NSIRC, Granta Park, Great Abington, Cambridge, CB21 6AL, UK.  
 james.campbell@brunel.ac.uk

**Abstract**— Previous work developed a particle-to-particle contact algorithm to treat frictionless sliding between two bodies discretised by SPH particles without the requirement to construct surfaces or approximate a surface normal. This algorithm was then extended to contact between finite element and SPH domains and has subsequently been extensively applied to a range of problems. This paper extends the particle-to-particle contact algorithm to include a friction model to broaden the applicability of the contact algorithm. A simple friction model based on a Coulomb formulation has implemented. This generates a lateral contact force between individual particle pairs, with the friction force vector being orthogonal to the local contact force vector. 2D and 3D sensitivity studies show that the friction model works effectively with the overall contact algorithm.

## I. INTRODUCTION

Effective and robust treatment of contact between deformable materials remains a challenge in computational mechanics. In the finite element method contact algorithms use the mesh geometry to define the external surface of a body in contact, with contact forces then calculated to enforce the contact condition. A particular challenge when treating contact with the SPH method is the definition of the contact surface and robust treatment of the interface geometry as the bodies in contact deform. One approach is to identify the particles that are on the boundary of a body and from them the local surface normal [1], contact forces can then be generated between these boundary particles. Experience with this approach led to the development of an alternative particle-to-particle approach where contact is treated as an interaction between a particle and all neighbor particles within its support domain that belong to a separate body [2]. This approach removes the requirement to identify boundary particles, or a surface normal, providing robust treatment of contact even with large material deformation. This approach was subsequently extended to the treatment of contact between SPH and finite element domains [3]. The contact treatment has been successfully applied to a range of applications including: impact on water and behavior of floating bodies [3-5]; bird strike [6] and ballistic impact [3]. In all these applications, friction between the bodies in contact can be neglected and the contact can be treated as frictionless. However there are many applications where this assumption is not valid.

This paper presents research towards extending the contact algorithm to include friction models. In this work a simple friction model, consistent with the particle-to-particle nature of the contact algorithm, has been implemented. Then a number of sensitivity studies to investigate the behavior of this friction model have been undertaken. The paper is organized as follows: the particle-to-particle contact algorithm is summarized in section 2. The simple

friction model is presented in section 3. Numerical results from sensitivity studies are presented in section 4.

## II. PARTICLE-TO-PARTICLE CONTACT

The contact algorithm is based on the use of a potential function defined as [2]:

$$\phi_c(x_i) = \int_{\Omega_c} K \left( \frac{W(x_i - x_j)}{W(h_{avg})} \right)^n dV, \quad (1)$$

where  $\Omega_c$  is the union of all bodies  $\Omega_k$  for which  $x_i \notin \Omega_k$ , and  $K$  and  $n$  are user defined parameters providing control over the magnitude and shape of the potential.  $W$  is the SPH interpolation kernel and  $h_{avg}$  is the average of the smoothing length at the two points. This potential function has the following properties:

- zero inside a domain,
- always positive or zero,
- increases as the distance between two bodies decreases.

By defining the contact force as the gradient of the potential field,

$$b_c = \nabla \phi_c, \quad (2)$$

the contact force appears in the conservation of momentum equation as:

$$\nabla \sigma + b_c = \rho a. \quad (3)$$

An SPH discretisation of (3) leads to an expression for the body force as a sum over contact neighbour particles:

$$b_c(x_i) = \sum_{j \in \Omega_c} \frac{m_j}{\rho_j} Kn \frac{W(x_i - x_j)^{n-1}}{W(h_{avg})^n} \nabla_{x_i} W(x_i - x_j). \quad (4)$$

Equation (4) allows the definition of a contact force vector  $\mathbf{f}_{ij}$  between particle  $i$  and a neighbour particle  $j$ , that is aligned with vector  $\mathbf{r}_{ij} = \mathbf{x}_i - \mathbf{x}_j$  between the particle centres:

$$\mathbf{f}_{ij} = \frac{m_j}{\rho_j} \frac{m_i}{\rho_i} Kn \frac{W(x_i - x_j)^{n-1}}{W(h_{avg})^n} \nabla_{x_i} W(x_i - x_j). \quad (5)$$

The individual force vectors can then be added to the contribution of the internal and external forces in the

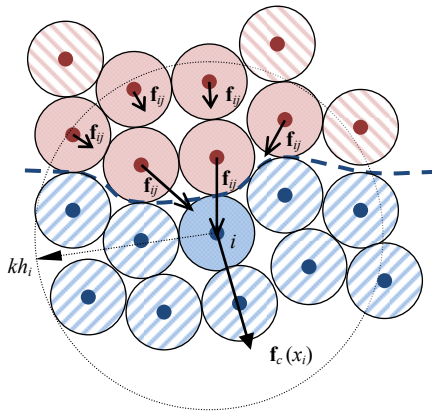


Figure 1. An illustration of particle-to-particle contact. A contact force,  $\mathbf{f}_{ij}$ , is generated between particle  $i$  and each neighbour particle in the second body (red). Together the individual inter-particle contact forces generate the total force on particle  $i$  due to contact,  $\mathbf{f}_c(x_i)$

momentum equation, with the resultant contact force at particle  $i$  then given by

$$\mathbf{f}_c(x_i) = \sum_{j \in \Omega_c} \mathbf{f}_{ij} \cdot \quad (6)$$

This is illustrated in fig. 1, where particle  $i$  interacts through the contact algorithm with all particles belonging to the second body that are within its support domain,  $kh_i$ .

### III. FRICTION MODEL

To investigate the compatibility of the particle-to-particle contact algorithm with friction models, a very simple friction model, based on Coulomb's Law of Friction was developed and implemented. This law defines the friction force,  $f_f$ , between two surfaces in contact as

$$f_f \leq \mu f_c \cdot \quad (7)$$

Where  $f_c$  is the normal force on each surface due to contact and  $\mu$  is the coefficient of friction, an empirical property of the surfaces in contact. The friction force always acts to oppose the relative motion of the two surfaces.

To preserve the particle-to-particle nature of the contact algorithm, a friction force is defined between each particle pair in contact, with the magnitude of the contact force,  $|\mathbf{f}_f|$ , related to the magnitude of the normal force,  $|\mathbf{f}_{ij}|$ , by the friction coefficient by:

$$|\mathbf{f}_f| = \mu |\mathbf{f}_{ij}| \cdot \quad (8)$$

The direction of the contact force is defined by the relative velocity vector,  $\mathbf{v}_{ij} = \mathbf{v}_i - \mathbf{v}_j$ , of the two particles. Combined with the inter-particle vector,  $\mathbf{r}_{ij}$ , the component of the relative velocity vector in the direction of the inter-particle vector can be written as:

$$\frac{\mathbf{r}_{ij}}{|\mathbf{r}_{ij}|} \left( \frac{\mathbf{r}_{ij} \cdot \mathbf{v}_{ij}}{|\mathbf{r}_{ij}|} \right) \cdot \quad (9)$$

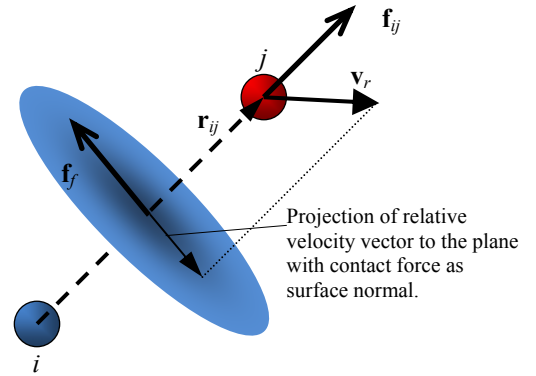


Figure 2. A diagram illustrating the definition of the friction force vector,  $\mathbf{f}_f$ . The force is normal to the inter-particle vector  $\mathbf{r}_{ij}$  and acts to oppose the relative velocity,  $\mathbf{v}_r$ .

Therefore the component of the inter-particle velocity normal to the inter-particle vector is

$$\mathbf{v}_n = \mathbf{v}_{ij} - \frac{\mathbf{r}_{ij}}{|\mathbf{r}_{ij}|} \left( \frac{\mathbf{r}_{ij} \cdot \mathbf{v}_{ij}}{|\mathbf{r}_{ij}|} \right) \cdot \quad (10)$$

The friction force vector is therefore

$$\mathbf{f}_f = -\frac{\mu |\mathbf{f}_{ij}|}{|\mathbf{v}_n|} \mathbf{v}_n \cdot \quad (11)$$

Equation (11) has been implemented in a 3D SPH code to allow the behaviour of this simple model to be investigated. In the current work no distinction is made between static and dynamic friction and the magnitude of the inter-particle friction force is always defined by (8), unless  $|\mathbf{v}_n| = 0$ . In that case the friction force is set to zero to prevent a floating-point division by zero error.

### IV. NUMERICAL RESULTS

A set of block sliding models in 2D and 3D are used to investigate the behaviour of the friction model. The purpose of these models is to investigate the ability of the model to simulate frictional contact and the influence of the relative distribution of the particles on the surfaces in contact on the sliding behaviour.

#### A. 2D sliding contact

The first investigation models the behaviour of a rectangular block sliding over a flat surface in 2D. The block is given an initial velocity parallel to the surface which should decrease under friction. A similar test has been used in a previous SPH contact investigation [7].

The model consists of a rectangular block, 1.0 m  $\times$  0.5 m, with an initial velocity of 2.0 m/s, fig. 3. The block is modelled as an elastic-plastic solid with density  $\rho = 7800$  kg/m<sup>3</sup>, Young's Modulus  $E = 210$  GPa, Poisson's ratio  $\nu = 0.3$  and yield stress 250 MPa. Although an elastic-plastic material model was used, the material remained elastic throughout all the simulations. Gravity is applied to all parts of the model, 9.81 m/s<sup>2</sup>, so contact forces result between the block and

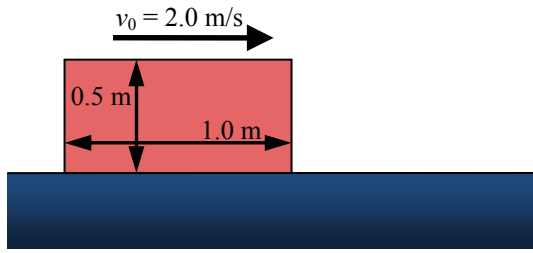


Figure 3. Layout of 2D sliding block test problem.

surface and the resulting friction forces generate a constant deceleration of the block. The overall motion of the block is easy to predict and its behaviour for friction coefficients from  $\mu = 0.0$  to  $\mu = 1.0$  was investigated.

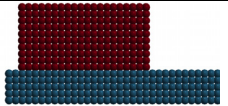
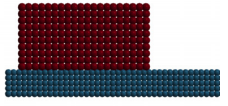
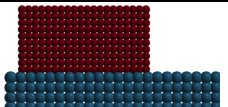
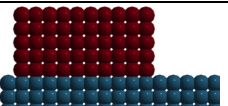
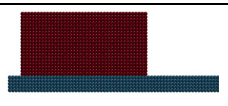
The reference model represents the block using 200 SPH particles in a  $10 \times 20$  cubic array, using the Total-Lagrangian form of SPH. The surface is represented by 5 layers of SPH particles, using identical material properties to the block. All particles on the bottom layer are fully constrained in translation. This condition approximates a rigid surface while ensuring that no particles included in the contact neighbourhood have translational constraints.

Velocity vs. time graphs for six values of the friction coefficient are shown in fig 4a. For frictionless contact the block slides at a constant velocity, while for friction the block decelerates to rest. The model behaviour agrees well with the predicted behaviour. The model results show an oscillation about the analytical results due to the particle-to-particle nature of the contact. The use of a contact potential means that the particle distributions in the bodies in contact influence the local contact forces, and as the two bodies have identical cubic packing this represents a worst case. This consequence is the variation in the velocity about a mean value as the two bodies slide. This local behaviour does not prevent correct overall behaviour of the block, fig.5.

To investigate the influence of the relative particle spacing four additional models were generated, as shown in table 1. In models 2 and 3 the block packing is unchanged from model 1, just the spacing of the surface is changed. Model 2 has a smaller inter-particle spacing and model 3 has a larger spacing. The resulting velocity vs. time curves, fig. 4b and fig. 4c respectively, show that with different spacing in the two bodies the oscillation in velocity is removed and the overall behaviour of the block agrees with the predicted solution. There is still local variation in the contact force as individual particles move relative to each other, but the resultant behaviour of all particles in contact approximates sliding friction well.

In the final two models, the overall particle spacing is changed in both block and surface. In model 4 the spacing is larger, with the block consisting of a  $5 \times 10$  particle array, while model 5 uses a  $20 \times 40$  particle array. The velocity vs. time curves for the two models are shown in fig. 4d and fig. 4e respectively. Both these models show the same oscillation in velocity, which is more pronounced in model 4 due to the larger particles.

TABLE I. DETAILS OF THE FIVE 2D BLOCK SLIDING MODELS TESTED.

Model	$\Delta p_{block}$ m	$\Delta p_{surface}$ m	Initial setup
1	0.05	0.05	
2	0.05	0.04	
3	0.05	0.075	
4	0.1	0.1	
5	0.025	0.025	

Overall these model results show that the simple friction model effectively represents the simple friction law implemented.

### B. Sliding from rest

This second test case was intended to investigate the ability of the algorithm to treat a body at rest and a subsequent transition to motion. Model 2 from the sliding tests was taken as the basis for this test case. In this case the block is initially at rest and the angle of the surface with respect to gravity is gradually increased. For frictionless sliding the block immediately begins to move, with acceleration increasing as the angle increases. For sliding with friction the block remains at rest until the angle reaches a critical value where the gravitational acceleration tangential to the surface overcomes the friction force and the block begins to move. To simplify the prediction of the motion, the change in slope angle is represented by changing the direction of the base acceleration vector, rather than actual rotation of the block and surface. In the test results shown here the rate of change of the base vector direction is  $45^\circ$  per second.

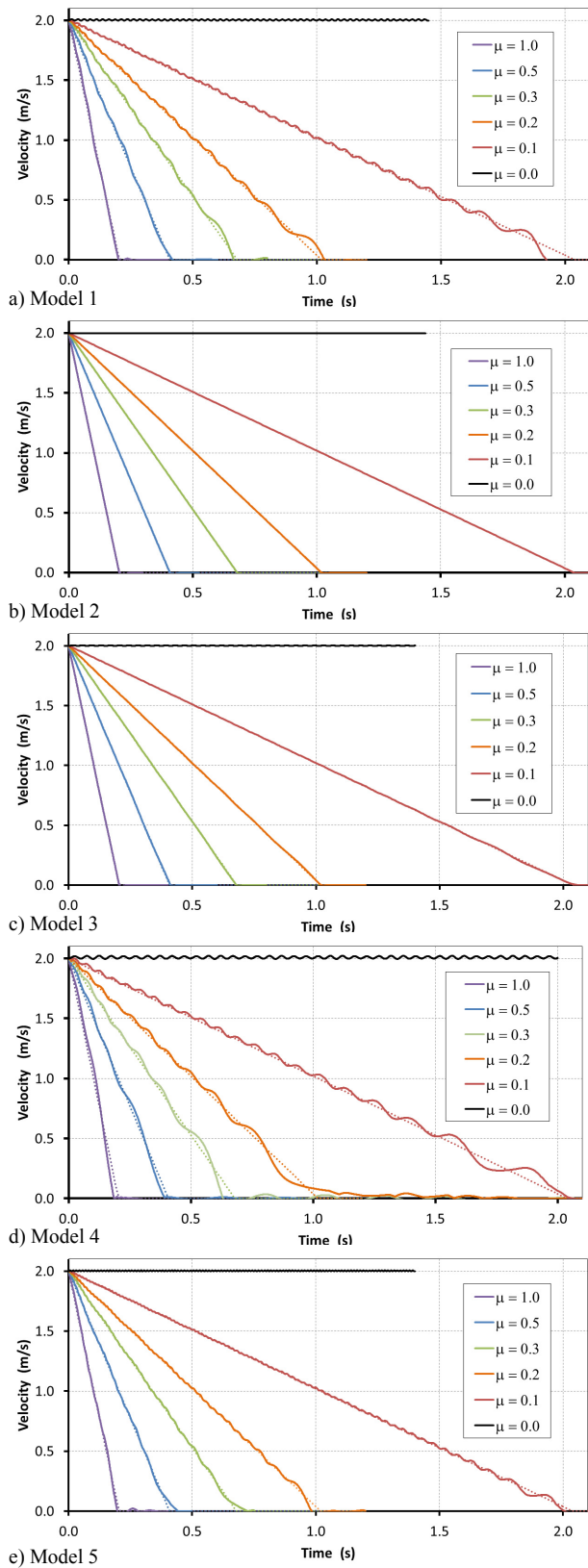


Figure 4: Graphs of velocity vs. time for varying coefficient of friction. Results for models 1 -5 are shown in graphs a – e respectively. For each case the solid line represents the numerical model results, and the dotted line represents the analytical solution.

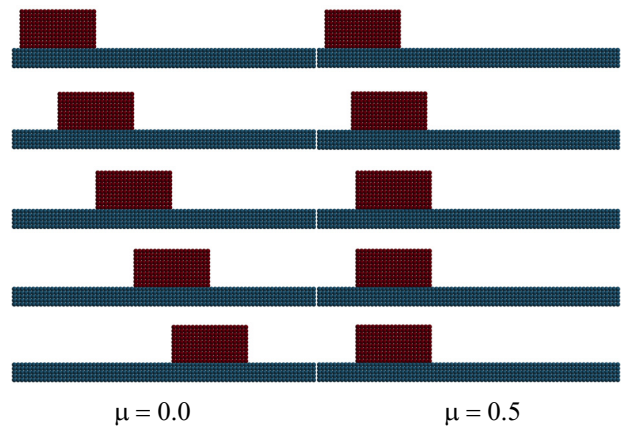


Figure 5. 2D sliding contact behaviour for frictionless sliding (left) and sliding with friction (right). The time interval between images is 0.25 s.

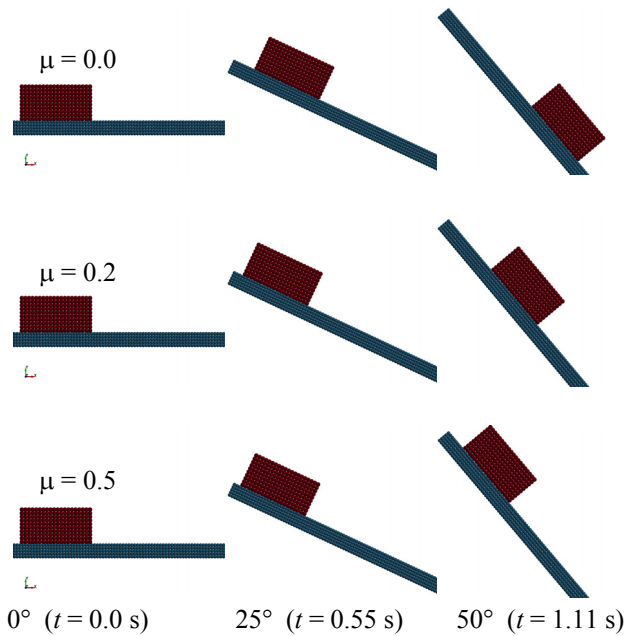


Figure 6. Sliding contact behaviour for block initially at rest for three values of friction coefficient. For each case the left image is the initial state, the centre is for 25° (t = 0.55 s) and the right is for 50° (t = 1.11 s).

Fig. 6 shows the resulting behaviour for three values of the friction coefficient. With friction present the block initially does not move, when accelerates once a critical angle is reached. Velocity vs. time curves are shown in fig. 7, demonstrating that the simple friction model behaves well in this test, although as the friction coefficient increases there is increasing error close to the critical angle.

### C. 3D sliding contact

To investigate that the behaviour in 3D is equivalent to the 2D results, a 3D sliding block problem was developed. The block is now 1.0 m × 1.0 m × 0.5 m, represented by a 20 × 20 × 10 particle array. The relative particle spacing is based on the 2D model 3 setup. The block is given an initial velocity of 2.0 m/s

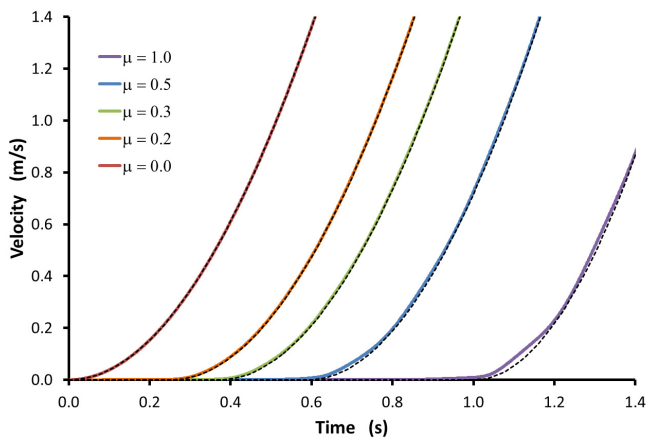


Figure 7. Graph of velocity vs. time for varying coefficient of friction for block initially at rest. The dashed lines are the analytic solutions for each case. The angle of the base acceleration representing gravity rotates at  $45^\circ$  per second.

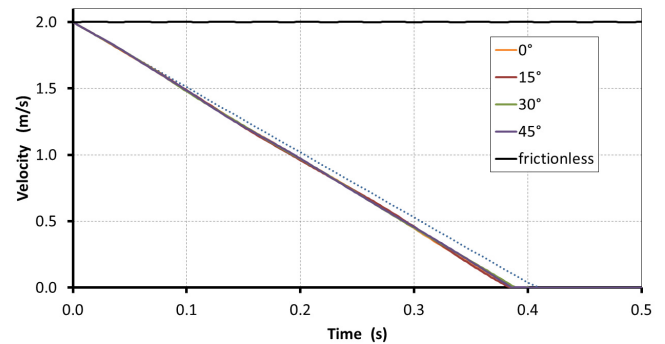


Figure 9. Graph of velocity vs. time for 3D sliding test. The friction coefficient is  $\mu = 0.5$  for all angles.

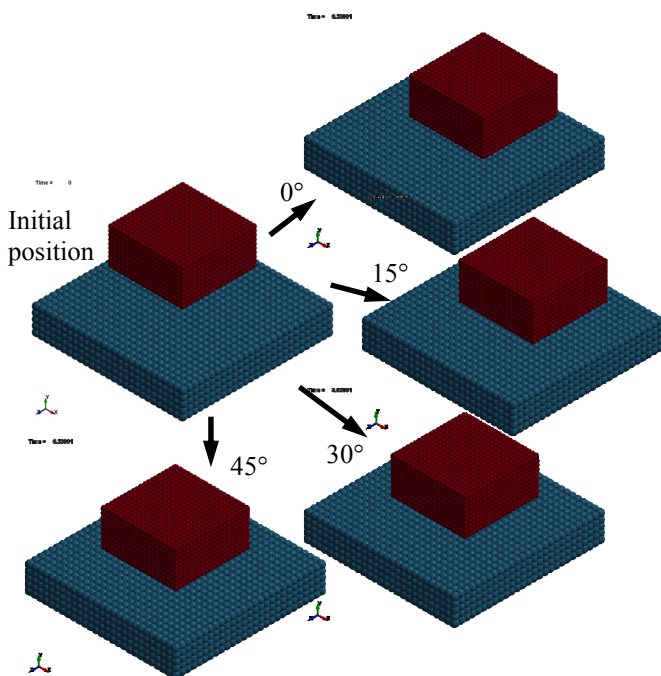


Figure 8. 3D sliding block behaviour showing the initial position for all models and the final position for each of the sliding angles.

parallel to the surface, but with different angles with respect to the cubic packing direction. Four angles have been investigated,  $0^\circ$ ,  $15^\circ$ ,  $30^\circ$  and  $45^\circ$  as shown in fig. 8. The velocity vs. time graphs for two friction coefficients ( $\mu = 0.0$  and  $\mu = 0.5$ ) are shown in fig. 9. The results show that for frictionless sliding the behaviour is equivalent to the 2D results. For sliding with friction the results show no significant validation with respect to direction over the surface, although the rate of deceleration is higher than expected, indicating the friction forces are too high and this requires further investigation.

## V. CONCLUSIONS

A simple friction model has been implemented in an existing particle-to-particle contact algorithm. Tests of the algorithm for sliding contact in 2D show that this approach can be used to represent frictional sliding behaviour in SPH models. Test results also show that the algorithm works effectively in 3D, although there is a small over estimation of the friction force that requires further investigation. Future development of the frictional contact algorithm is necessary to permit general use, this will concentrate in the treatment of sticking contact and the transition to motion.

## ACKNOWLEDGEMENT

The project leading to this publication has been part-funded by the European Union's Horizon 2020 research and innovation programme under grant agreement No 636549.

## REFERENCES

- [1] J.C. Campbell, R. Vignjevic, and L. Libersky. "A Contact Algorithm for Smoothed Particle Hydrodynamics," *Computer Methods in Applied Mechanics and Engineering*, vol. 181, pp. 49-56, 2000.
- [2] R. Vignjevic, T. De Vuyst, and J.C. Campbell. "A frictionless contact algorithm for meshless methods," *Computer Modeling In Engineering & Sciences*. Vol. 13, pp. 35-48, 2006.
- [3] T. De Vuyst, R. Vignjevic, and J.C. Campbell. "Coupling between meshless and finite element methods," *International Journal of Impact Engineering*, vol. 31, pp. 1054-1064, 2005.
- [4] J.C. Campbell, and R. Vignjevic, "Simulating structural response to water impact," *International Journal of Impact Engineering*, vol. 49, pp. 1-10, 2012.
- [5] M.H. Patel, R. Vignjevic, and J.C. Campbell. "An SPH technique for evaluating the behaviour of ships in extreme ocean waves," *International Journal of Maritime Engineering*, vol. 151, pp.39-47, 2009.
- [6] R. Vignjevic, M. Orłowski, T. De Vuyst, and J.C. Campbell, "A parametric study of bird strike on engine blades," *International Journal of Impact Engineering*, vol. 60, pp. 44-57, 2013.
- [7] D. Munro, "Towards a rigorous derivation of a stable and consistent smoothed particle hydrodynamics method", PhD Thesis, Cranfield University, 2015.